

## Quantum mechanical and electrochemical investigations on corrosion inhibition properties of novel heterocyclic Schiff bases

Nimmy Kuriakose, K. Joby Thomas\*, Vinod P. Raphael and C. Sini Varghese

Research Division, Department of Chemistry, St.Thomas' College (University of Calicut) Thrissur, Kerala, India

### CHRONICLE

#### Article history:

Received January 2, 2017

Received in revised form

March 1, 2017

Accepted April 21, 2017

Available online

April 22, 2017

#### Keywords:

Corrosion inhibitors

Mild Steel

Schiff base

Electrochemical impedance

Polarization studies

### ABSTRACT

The corrosion inhibition efficiencies of two novel Schiff bases, namely (E)-3-[thiophen-2-ylmethyleneamino]benzoic acid (T2YMABA) and (E)-4-(5-[(2-phenylhydrazono)methyl]thiophen-2-yl)benzoic acid (PHMT2YBA) on mild steel (MS) in 1.0M HCl solution has been investigated and compared using electrochemical impedance spectroscopy and potentiodynamic polarization analysis. The Schiff bases exhibited very good corrosion inhibitions on mild steel in 1.0M HCl medium and the inhibition efficiency increased with the increase in concentration of the inhibitor. Polarization studies revealed that T2YMABA acted as a mixed type inhibitor whereas PHMT2YBA molecules acted as anodic inhibitor.

© 2017 Growing Science Ltd. All rights reserved.

## 1. Introduction

Nitrogen containing organic compounds exhibit excellent corrosion inhibition characteristics in acid medium. The presence of hetero atoms makes these inhibitors environmental friendly due to high chemical activity and low toxicity<sup>1-3</sup>. Despite the large numbers of organic compounds, several Schiff bases were considered as good corrosion inhibitors. The presence of C=N- group and electronegative N, S or O atoms in the molecule give remarkable corrosion inhibition properties<sup>4-6</sup>. The specific interaction developed between the functional groups and the metal surface adds to the inhibition capacity of these molecules. Corrosion commonly occurs at metal surfaces in the presence of oxygen and moisture, involving electrochemical reactions<sup>7,8</sup>. The application of Schiff bases as an effective corrosion inhibitor is mainly based on their ability to form a monolayer on the surface of the corroding material. Electrochemical investigations can be employed to study the corrosion behaviour of metals and mechanism of inhibition of these Schiff bases<sup>9-11</sup>.

The present investigation was undertaken to examine the corrosion inhibition behaviours of two novel heterocyclic Schiff bases T2YMABA and PHMT2YBA. The anticorrosive activities of these compounds were evaluated by electrochemical impedance spectroscopy (EIS) and potentiodynamic

\* Corresponding author. Tel.: +919847177695

E-mail address: [drjobythomask@gmail.com](mailto:drjobythomask@gmail.com) (K. J. Thomas)

© 2017 Growing Science Ltd. All rights reserved.

doi: 10.5267/j.ccl.2017.6.001

polarization analysis. Quantum chemical studies were also conducted to study the corrosion inhibition response of these organic molecules which can be correlated with the energy of frontier molecular orbitals<sup>12-14</sup>.

## 2. Results and discussions

### 2.1 Quantum chemical calculations

The corrosion inhibitive properties of the inhibitor molecules can be well studied by analysing the energy levels of frontier molecular orbitals. The interaction between the vacant d orbitals of atoms on the Iron surface and the filled molecular orbitals of the inhibitor molecules can be considered as a donor-acceptor type according to the HSAB concept. This interaction plays the prominent role in the prevention of metallic corrosion. A strong binding between the inhibitor molecules and the metal surface is indicated by the larger value of  $E_{\text{HOMO}}$ . The energy difference between the HOMO and LUMO ( $\Delta E$ ) should be the lowest in that case<sup>15</sup>. GAMMES software and DFT method are employed for the optimization of geometry of molecules and quantum chemical calculations. A combination of Beck's three parameter exchange functional and Lee–Yang–Parr nonlocal correlation functional (B3LYP) was used in DFT calculations<sup>16</sup>. Quantum mechanical parameters like  $E_{\text{HOMO}}$ ,  $E_{\text{LUMO}}$  and  $\Delta E$  for the studied inhibitors are given in Table 1. HSAB parameters like chemical hardness ( $\eta$ ) and electronegativity ( $\chi$ ) of the molecules were calculated by the following equations<sup>17</sup>,

$$\chi \approx -1/2 (E_{\text{HOMO}} + E_{\text{LUMO}}), \quad (1)$$

$$\eta \approx 1/2 (E_{\text{HOMO}} - E_{\text{LUMO}}). \quad (2)$$

The  $E_{\text{HOMO}}$  value of the PHMT2YBA molecule was found to be higher among the two. Since the energy separation between HOMO and LUMO was also lower for PHMT2YBA than T2YMABA, it can be inferred that PHMT2YBA has a better inhibition activity than the other. Lower energy is required to render electrons from HOMO of PHMT2YBA to the vacant d-orbitals of Fe. The probability of acceptance of electrons from the metal surface to the LUMO of lowest energy of the inhibitor is the greatest. The number of electrons ( $\Delta N$ ) transferred from donor to acceptor molecules are calculated from the quantum chemical parameters. As an approximation, the chemical hardness of Fe bulk metal is assumed as zero and the approximate electronegativity of bulk Fe is taken as 7eV. The approximate number of electron transferred from the inhibitor molecule to the Fe atoms is calculated by the following equation,

$$\Delta N = \frac{\chi_{\text{Fe}} - \chi_{\text{inhib}}}{2(\eta_{\text{Fe}} + \eta_{\text{inhib}})}. \quad (3)$$

It is evident that the number of electrons transferred from the inhibitor molecule to the acceptor atom is greater for PHMY2BA, which suggests that this molecule make a strong coordinate type interaction with the metal atoms. The HOMO and LUMO of the molecules are represented in the Fig. 1.



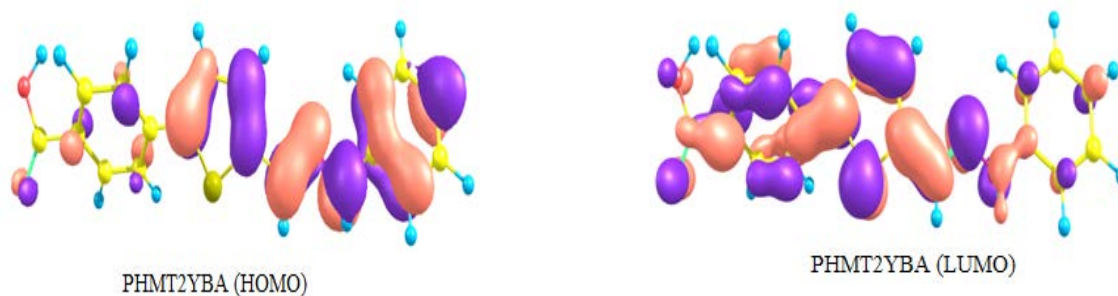


**Fig. 1.** HOMO and LUMO of T2YMABA and PHMT2YBA

**Table 1.** Quantum chemical parameters of T2YMABA and PHMT2YBA

Molecule	$E_{\text{HOMO}}$ (eV)	$E_{\text{LUMO}}$ (eV)	$\Delta E$ (eV)	$\chi$	$\eta$	$\Delta N$
T2YMABA	-4.0599	0.2258	4.2857	1.9171	2.1428	1.1860
PHMT2YBA	-3.4749	0.5306	4.0055	1.4722	2.0028	1.3801

## 2.2. Electrochemical impedance spectroscopy

Fig. 3 and Fig. 4 represent the Nyquist and Bode plots of MS specimens in the presence and absence of the inhibitors T2YMABA and PHMT2YBA in 1.0 M HCl. It is evident from the plots that the impedance response of metal specimens showed a marked difference in the presence and absence of the inhibitors. The capacitance loop intersects the real axis at higher and lower frequencies. At high frequency end, the intercept corresponds to the solution resistance ( $R_s$ ) and at lower frequency end, corresponds to the sum of  $R_s$  and charge transfer resistance ( $R_{ct}$ ). The difference between the two values gives  $R_{ct}$ <sup>18-20</sup>. The value of  $R_{ct}$  is a measure of electron transfer across the exposed area of the metal surface and it is inversely proportional to rate of corrosion<sup>21-23</sup>.

Impedance behavior can be well explained by pure electric models that could verify and enable to calculate numerical values corresponding to the physical and chemical properties of electrochemical system under examination. The simple equivalent circuit that fit to many electrochemical system composed of a double layer capacitance,  $R_s$  and  $R_{ct}$ <sup>24,25</sup>. To reduce the effects due to surface irregularities of metal, constant phase element (CPE) is introduced into the circuit instead of a pure double layer capacitance<sup>26</sup> which gives more accurate fit as represented in Fig. 2. The impedance of CPE can be expressed as

$$Z_{\text{CPE}} = \frac{1}{Y_0 (j\omega)^n}, \quad (4)$$

where  $Y_0$  is the magnitude of CPE,  $n$  is the exponent (phase shift),  $\omega$  is the angular frequency and  $j$  is the imaginary unit. CPE may be resistance, capacitance and inductance depending upon the values of  $n$ <sup>27</sup>. In all experiments the observed value of  $n$  ranges between 0.8 and 1.0, suggesting the capacitive response of CPE.

The EIS parameters such as  $R_{ct}$ ,  $R_s$  and CPE and the calculated values of percentage of inhibition ( $\eta_{\text{EIS}}\%$ ) of MS specimens are listed in Table 2. The  $R_{ct}$  values are increased with increasing inhibitor concentration. Decrease in capacitance values CPE with inhibitor concentration can be attributed to the decrease in local dielectric constant and /or increase in the thickness of the electrical double layer. This emphasis the action of inhibitor molecules by adsorption at the metal–solution interface<sup>28</sup>. The percentage of inhibition ( $\eta_{\text{EIS}}\%$ ) showed a regular increase with increase in inhibitor concentration. A maximum of 94.34% and 96.83% inhibition efficiencies were achieved at an inhibitor concentration of 1mM for T2YMABA and PHMT2YBA.

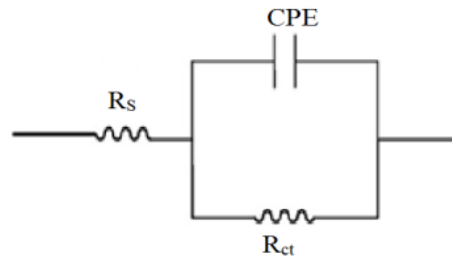


**Fig. 2.** Equivalent circuit model

**Table 2.** Electrochemical impedance parameters in the presence and absence of Schiff base inhibitors T2YMABA and PHMT2YBA in 1.0 M HCl

Inhibitors	C	C <sub>dl</sub>	R <sub>ct</sub>	$\eta_{EIS}\%$
T2YMABA	0	95.8	16.4	-
	0.2	73.4	70.3	76.07
	0.4	120	86.7	81.08
	0.6	111	117	85.99
	0.8	77.5	238	93.11
	1.0	91.7	290	94.34
PHMT2YBA	0.2	79	68.9	76.19
	0.4	113	79.6	79.39
	0.6	63.7	174	90.57
	0.8	75.6	176	90.68
	1.0	69.6	317	96.83

### 2.3. Potentiodynamic polarization studies

Potentiodynamic polarization curves for the inhibitors T2YMABA and PHMT2YBA are shown in Fig. 5 and Fig. 6, respectively. Polarization parameters like corrosion current densities ( $I_{corr}$ ), corrosion potential ( $E_{corr}$ ), cathodic Tafel slope ( $b_c$ ), anodic Tafel slope ( $b_a$ ), and inhibition efficiency ( $E_p$ ) for MS specimens are listed in Table 3.

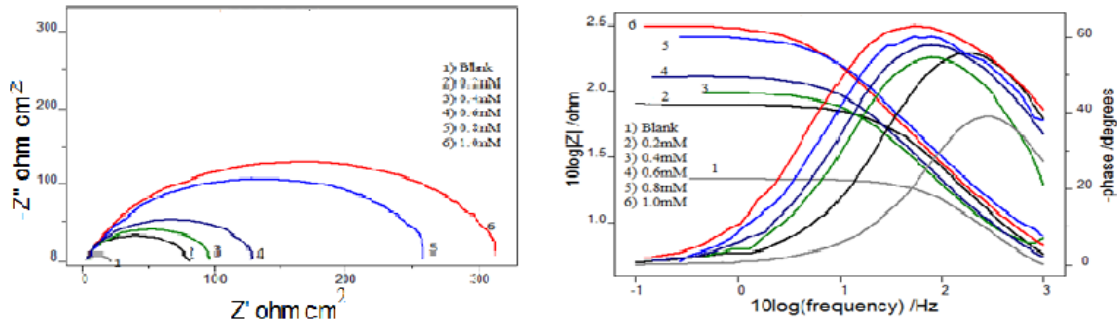


**Fig. 3.** Nyquist and Bode plots in the presence and absence of T2YMABA in 1.0 M HCl

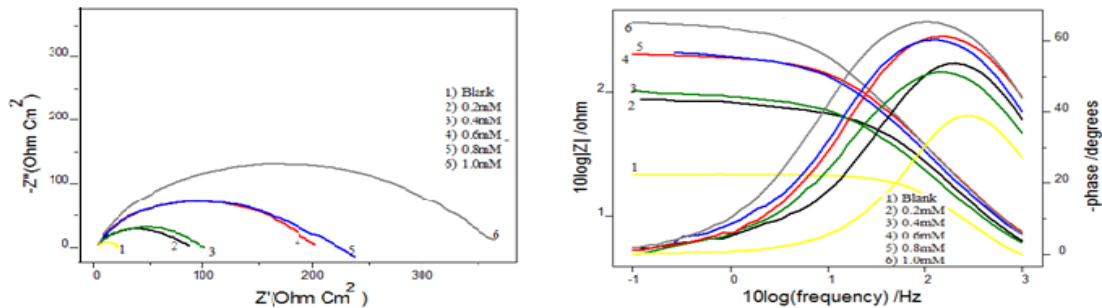


**Fig. 4.** Nyquist and Bode plots in the presence and absence of PHMT2YBA in 1.0 M HCl

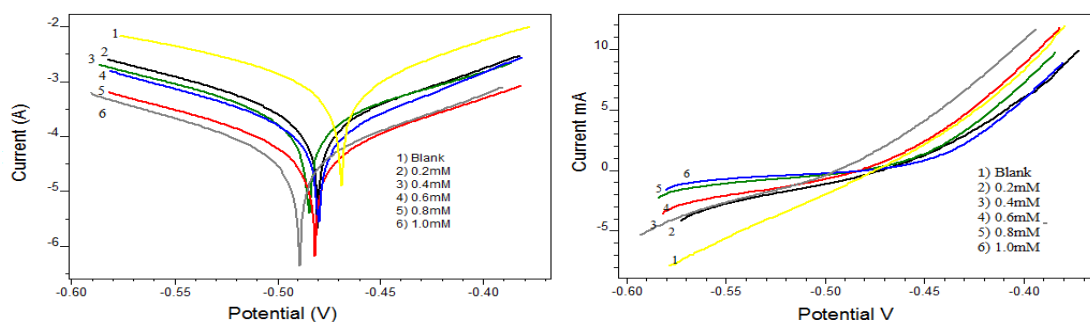


**Fig. 5.** Tafel and Linear polarization plots in the presence and absence of T2YMABA in 1.0 M HCl

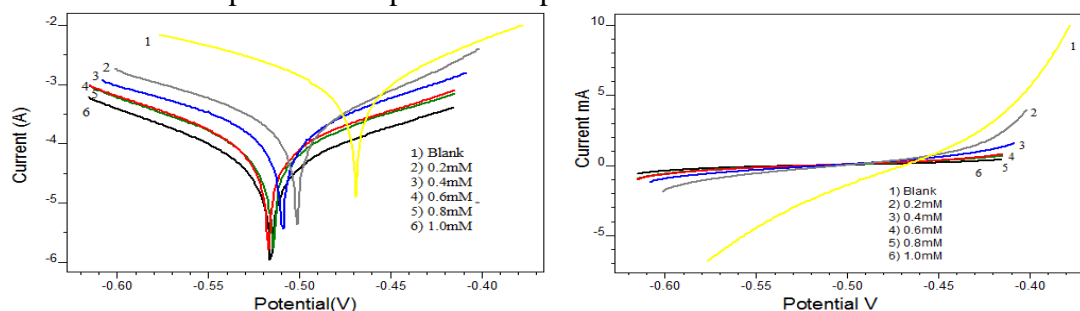


**Fig. 6.** Tafel and Linear polarization plots in the presence and absence of PHMT2YBA in 1.0 M HCl

A prominent decrease in the corrosion current density ( $I_{\text{corr}}$ ) was observed in the presence of inhibitors. A lowest value of  $I_{\text{corr}}$  was noticed for the inhibitor solution of concentration 1mM which exhibited a maximum inhibition efficiency of 94.07% and 96.62% for T2YMABA and PHMT2YBA respectively. On evaluation of the Tafel and polarization curves, one can see that slope of the Tafel lines in presence of inhibitor varied considerably compared to the Tafel lines of uninhibited solution. The inhibitor can be regarded as mixed type inhibitors since the slopes of both Tafel lines are affected considerably. If the anodic or cathodic slopes vary from the slope of the uninhibited solution, the inhibitor can be treated as an anodic or cathodic type inhibitor<sup>7</sup> Since the value of  $b_a$  changes appreciably in the presence of inhibitors, it may be assumed that the inhibitor molecules are more adsorbed on anodic sites. Generally if the shift of  $E_{\text{corr}}$  is  $>85$  with respect to  $E_{\text{corr}}$  of uninhibited solution, the inhibitor can be viewed as cathodic or anodic type<sup>29</sup>. For the inhibitor T2YMABA the cathodic slope is slightly varied suggesting that these molecules are acting on both the cathode and anode and thus can be regarded as a mixed type inhibitor. Whereas PHMT2YBA molecules acted as anodic inhibitor for MS specimens in 1.0 M HCl<sup>30</sup>.

**Table 3.** Potentiodynamic polarization parameters in the presence and absence of Schiff base inhibitors T2YMABA and PHMT2YBA in 1.0 M HCl

Inhibitor	Tafel Data					Linear polarization data		
	C (mM)	$-E_{\text{corr}}$ (mV/SCE)	$I_{\text{corr}}$ ( $\mu\text{A}/\text{cm}^2$ )	$-b_c$ (mV/dec)	$b_a$ (mV/dec)	$\eta_{\text{pol}}\%$	$R_p$ (ohm)	$\eta_{\text{Rp}}\%$
T2YMABA	0	465	726	106	72	-	38	-
	0.2	476	183	89	79	74.79	82	73.51
	0.4	483	174	93	89	76.03	114	80.88
	0.6	475	111	90	68	84.71	152	85.66
	0.8	479	49.2	89	79	93.22	313	93.04
	1.0	487	40.4	86	76	94.44	367	94.07
PHMT2YBA	0.2	501	173	83	74	76.17	86	74.79
	0.4	500	131	81	91	81.96	125	82.62
	0.6	517	76	84	100	89.53	214	89.81
	0.8	515	68	76	94	90.63	221	90.14
	1.0	516	39	85	95	94.63	405	96.62

## 2.4 Surface morphological studies

SEM images of mild steel specimens were taken to ascertain the mechanism of action of Schiff base inhibitors on the metal surface. Fig. 7 shows the SEM images of bare MS surface, MS specimen in 1.0 M HCl and MS specimen in 1.0M HCl containing T2YMABA with 1.0 mM concentration. The irregularities on the bare metal surface are due to the effect of surface polishing. It can be well understood that the metal surface is less damaged in the presence of inhibitor which is due to the formation of a protective film through adsorption on metal surface and thereby suppressing the rate of corrosion.

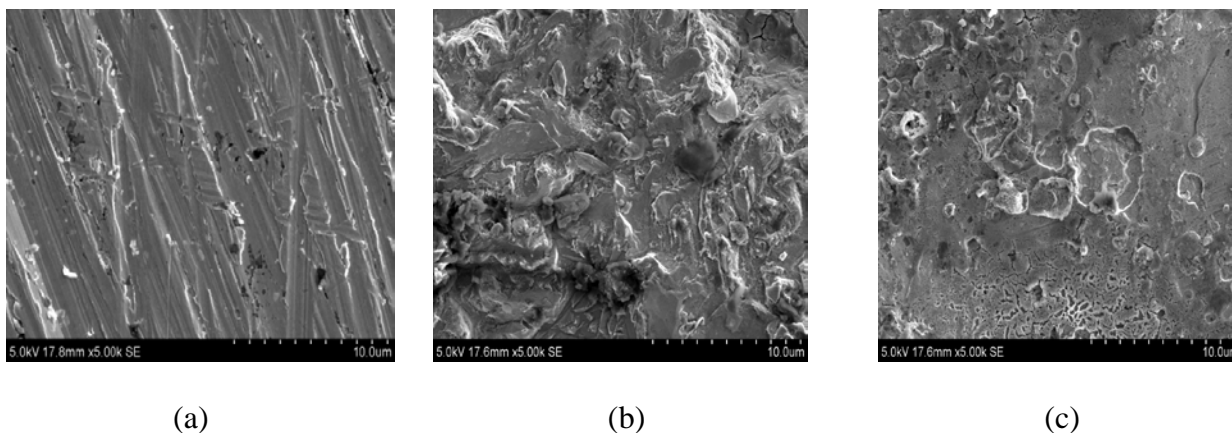


**Fig. 7.** SEM image of a) bare MS surface ,b) in 1.0 M HCl (blank) c) in 1.0M HCl and T2YMABA(1.0mM)

## 3. Conclusions

The relative inhibition efficiencies of two Schiff bases were studied in 1.0 M HCl solution. Both the inhibitors showed very high inhibitive efficiencies for mild steel in 1.0 M hydrochloric acid. The percentage inhibitive efficiency increases with increase in concentration. It is well known that the surface of the metal is positively charged in acidic media. The  $\text{Cl}^-$  ions could be specifically adsorbed on the metal surface and creates an excess of negative charge on the surface. This will favour the adsorption of protonated Schiff base on the surface and hence reduce the dissolution of Fe to  $\text{Fe}^{2+}$ . Besides this electrostatic interaction between the protonated Schiff base and the metal surface, other possible interactions are i) interaction of unshared electron pairs in the molecule with the metal ii) interaction of  $\pi$ -electrons with the metal and iii) a combination of types (i–ii)<sup>32-34</sup>. If one examines the structures of Schiff bases, many potential sources of inhibitor–metal interaction can be recognized. The unshared pair of electrons present on N atoms is of key importance in making coordinate bond with the metal. The  $\pi$ -electron cloud of the aromatic rings and the azomethine linkage also participate in the inhibition mechanism. Furthermore, the double bonds in the inhibitor molecule permit the back donation of metal d electrons to the  $\pi^*$  orbital and this type of interaction cannot occur with amines<sup>35</sup>.

## Acknowledgement

Authors are grateful to UGC for providing the financial assistance for the research work.

## 4. Experimental

### 4.1. Inhibitor

Two novel heterocyclic Schiff bases namely, (E)-3-[thiophen-2-ylmethyleneamino]benzoic acid (T2YMABA) and (E)-4-(5-[(2-phenylhydrazono) methyl]thiophen-2-yl)benzoic acid (PHMT2YBA) were prepared. The former one was derived from equimolar mixture of thiophene-2-carbaldehyde and 3-aminobenzoic acid in ethanol medium and the latter from 4-(5-formylthiophen-2-yl)benzoic acid and

phenylhydrazine by refluxing in ethanol medium. Fig. 8 represents the molecular structures of the heterocyclic Schiff bases T2YMABA and PHMT2YBA. Anal. calcd. for T2YMABA (C<sub>12</sub>H<sub>9</sub>NO<sub>2</sub>S): C, 63.84; H, 3.81; N, 7.04; S, 14.11%. IR (KBr) :  $\nu_{C=N}$  1579cm<sup>-1</sup>, <sup>1</sup>Hnmr:  $\delta_{COOH}$  12.93,  $\delta_{CH=N}$  3.25, <sup>13</sup>Cnmr:  $\delta_{COOH}$  167.03,  $\delta_{CH=N}$  154.99. Anal. calcd. for PHMT2YBA (C<sub>18</sub>H<sub>14</sub>N<sub>2</sub>O<sub>2</sub>S): C, 66.98; H, 4.06; N, 9.58; S, 8.99%. IR (KBr) :  $\nu_{C=N}$  1618cm<sup>-1</sup>, <sup>1</sup>Hnmr:  $\delta_{COOH}$  12.93,  $\delta_{CH=N}$  10.40, <sup>13</sup>Cnmr:  $\delta_{COOH}$  131.42,  $\delta_{CH=N}$  127.80.



**Fig. 8.** Molecular structure of T2YMABA and PHMT2YBA

#### 4.2. Solution

The aggressive solution of 1.0 M HCl was prepared by dilution of A.R grade (Merck) 37% of HCl with de-ionized water. Inhibitor solutions were prepared in the range 0.1mM-1mM concentrations.

#### 4.3. Quantum chemical studies

Optimization of geometry of molecules and quantum chemical calculations were performed by DFT method using GAMMES software. A combination of Beck's three parameter exchange functional and Lee–Yang–Parr nonlocal correlation functional (B3LYP) was employed in DFT calculations.

#### 4.4. Electrochemical impedance spectroscopy (EIS)

The EIS measurements were performed in a three electrode assembly. Saturated calomel electrode (SCE) was used as the reference electrode. Platinum electrode having 1cm<sup>2</sup> area was taken as counter electrode. Metal specimens with an exposed area of 1cm<sup>2</sup> were used as the working electrode. The EIS experiments were carried out on an Ivium compactstat-e electrochemical system. 1.0 M HCl was taken as the electrolyte and the working area of the metal specimens were exposed to the electrolyte for 1 h prior to the measurement. EIS measurements were performed at constant potential (OCP) in the frequency range from 1 KHz to 100 mHz with amplitude of 10 mV as excitation signal. The percentage of inhibitions from impedance measurements were calculated using charge transfer resistance values by the following expression<sup>2</sup>

$$\eta_{EIS} \% = \frac{R_{ct} - R'_{ct}}{R_{ct}} \times 100, \quad (5)$$

where  $R_{ct}$  and  $R'_{ct}$  are the charge transfer resistances of working electrode with and without inhibitor respectively.

#### 4.5. Potentiodynamic polarization

Electrochemical polarization studies were performed by recording anodic and cathodic potentiodynamic polarization curves. Polarization plots were obtained in the electrode potential range from -100 to +100 mV Vs corrosion potential ( $E_{corr}$ ) at a scan rate of 1mV/sec. Tafel polarization analysis were done by extrapolating anodic and cathodic curves to the potential axis to obtain corrosion current densities ( $I_{corr}$ ). The percentage of inhibition efficiency ( $\eta_{pol}\%$ ) was evaluated from the measured  $I_{corr}$  values using the following relation

$$\eta_{\text{pol}} \% = \frac{I_{\text{corr}} - I'_{\text{corr}}}{I_{\text{corr}}} \times 100, \quad (6)$$

where  $I_{\text{corr}}$  and  $I'_{\text{corr}}$  are the corrosion current densities of the exposed area of the working electrode in the absence and presence of inhibitor respectively. From the slope analysis of the linear polarization curves in the vicinity of corrosion potential of blank and different concentrations of the inhibitor, the values of polarization resistance ( $R_p$ ) in 1.0 M HCl solution were obtained. From the evaluated polarization resistance, the inhibition efficiency was calculated using the relationship

$$\eta_{R_p} \% = \frac{R'_p - R_p}{R'_p} \times 100, \quad (7)$$

where  $R'_p$  and  $R_p$  are the polarization resistance in the presence as well as the absence of the inhibitor, respectively <sup>2</sup>.

## References

1. Bentiss, F., Traisnel, M., Gengembre, L., and Lagrenée, M. (2000) Inhibition of acidic corrosion of mild steel by 3,5-diphenyl-4H-1,2,4-triazole. *Appl. Surf. Sci.*, 161(2), 194–202.
2. Raman, A. and Labine, P. (1986) *Reviews on Corrosion Inhibitor Science and Technology*, NACE, Houston, Tex, USA.
3. Oguzie, E.E. (2005) Corrosion inhibition of mild steel in hydrochloric acid solution by methylene blue dye. *Mat. Lett.*, 59(8) 1076-1079.
4. Yurt, A., & Aykın, Ö. (2011) Diphenolic Schiff bases as corrosion inhibitors for aluminium in 0.1 M HCl: Potentiodynamic polarisation and EQCM investigations, *Corros. Sci.*, 53(1) 68-76.
5. Li, X., Deng, S., & Fu, H. (2010) Blue tetrazolium as a novel corrosion inhibitor for cold rolled steel in sulphuric acid solution. *Mater. Chem. Phys.*, 129(30) 696-700.
6. Behpour, M., Ghoreishi, S. M., Soltani, N., Salavati-Niasari, M., Hamadani, M., & Gandomi, A. (2008) Electrochemical and theoretical investigation on the corrosion inhibition of mild steel by thiosalicylaldehyde derivatives in hydrochloric acid solution. *Corros. Sci.*, 50(8) 2172-2181.
7. Jacob, K. S., & Parameswaran, G. (2010) Corrosion inhibition of mild steel in hydrochloric acid solution by Schiff base furoin thiosemicarbazone. *Corros. Sci.*, 52(1) 224-228.
8. Deng, S., Li, X., & Fu, H. (2011) Alizarin violet 3B as a novel corrosion inhibitor for steel in HCl, H<sub>2</sub>SO<sub>4</sub> solutions. *Corros. Sci.*, 5(11) 3596-3602.
9. Paul, A., Thomas, K. J., Raphael, V. P., & Shaju, K. S. (2012) Chelating efficacy and corrosion inhibition capacity of Schiff base derived from 3-formylindole. *Orient. J. Chem.*, 28 (30) 1501-1507.
10. Raphael, V. P., Thomas, K. J., Shaju, K. S., & Paul, A. (2014) Corrosion inhibition investigations of 3-acetylpyridine semicarbazone on carbon steel in hydrochloric acid medium. *Res. Chem. Intermed.*, 40(8), 2689-2701.
11. Sethi, T., Chaturvedi, A., Upadhyay, R. K., & Mathur, S. P. (2007) Corrosion inhibitory effects of some Schiff's bases on mild steel in acid media. *J. Chil. Chem. Soc.*, 52(3) 1206–1213.
12. Bereket, G., Öğretir, C., & Yurt, A. (2001) Quantum mechanical calculations on some 4-methyl-5-substituted imidazole derivatives as acidic corrosion inhibitor for zinc. *J. Molec. Struct.: THEOCHEM*, 571(1-3) 139-145.
13. Khalil, N. (2003) Quantum chemical approach of corrosion inhibition. *Electrochim. Acta*, 48(18) 2635-2640.
14. Obot, I. B., & Obi-Egbedi, N. O. (2010) Adsorption properties and inhibition of mild steel corrosion in sulphuric acid solution by ketoconazole: experimental and theoretical investigation. *Corros. Sci.*, 52(1) 198-204.
15. Zhang, J., Liu, J., Yu, W., Yan, Y., You, L., & Liu, L. (2010) Molecular modeling of the inhibition mechanism of 1-(2-aminoethyl)-2-alkyl-imidazoline. *Corros. Sci.*, 52(6) 2059-2065.



16. Ashassi-Sorkhabi, H., Shaabani, B., & Seifzadeh, D. (2005) Effect of some pyrimidinic Schiff bases on the corrosion of mild steel in hydrochloric acid solution. *Electrochim. Acta*, 50 (16-17) 3446-3452.
17. Ferreira, E. S., Giacomelli, C., Giacomelli, F. C., & Spinelli, A. (2004). Evaluation of the inhibitor effect of L-ascorbic acid on the corrosion of mild steel. *Mater. Chem. Phys.*, 83(1) 129-134.
18. Li, X., Deng, S., & Fu, H. (2009) Synergism between red tetrazolium and uracil on the corrosion of cold rolled steel in H<sub>2</sub>SO<sub>4</sub> solution. *Corros. Sci.*, 51(6) 1344–1355.
19. Cano, E., Polo, J. L., La Iglesia, A., & Bastidas, J. M. (2004) A study on the adsorption of benzotriazole on copper in hydrochloric acid using the inflection point of the isotherm. *Adsorption*, 10(3) 219-225.
20. Hassan, H. H., Abdelghani, E., & Amin, M. A. (2007) Inhibition of mild steel corrosion in hydrochloric acid solution by triazole derivatives: Part I. Polarization and EIS studies. *Electrochim. Acta*, 52(22) 6359-6366.
21. Mansfeld, F. (1981) Recording and analysis of AC impedance data for corrosion studies. *Corrosion*, 37(5) 301-307.
22. Abdel-Aal, M. S., & Morad, M. S. (2001) Inhibiting effects of some quinolines and organic phosphonium compounds on corrosion of mild steel in 3M HCl solution and their adsorption characteristics. *Brit. J. Corros.*, 36(4) 253-260.
23. Bommersbach, P., Alemany-Dumont, C., Millet, J. P., & Normand, B. (2005) Formation and behaviour study of an environment-friendly corrosion inhibitor by electrochemical methods. *Electrochem. Acta*, 51(6) 1076-1084.
24. Rosenfield, I.L. (1981) *Corros. Inhibitors*, McGraw-Hill, New York, 66.
25. El Azhar, M., Mernari, B., Traisnel, M., Bentiss, F., & Lagrenee, M. (2001) Corrosion inhibition of mild steel by the new class of inhibitors [2, 5-bis (n-pyridyl)-1, 3, 4-thiadiazoles] in acidic media. *Corros. Sci.*, 43(12) 2229–2238.
26. Yurt, A., Balaban, A., Kandemir, S. U., Bereket, G., & Erk, B. (2004) Investigation on some Schiff bases as HCl corrosion inhibitors for carbon steel. *Mater. Chem. Phys.*, 85(2-3) 420–426.
27. Singh, A. K., Shukla, S. K., Singh, M., & Quraishi, M. A. (2011) Inhibitive effect of ceftazidime on corrosion of mild steel in hydrochloric acid solution. *Mater. Chem. Phys.*, 129(1) 68-76.
28. McCafferty, E., & Hackerman, N. (1972) Double layer capacitance of iron and corrosion inhibition with polymethylene diamines. *J. Electrochem. Soc.*, 119(2) 146-154.
29. Bentiss, F., Lebrini, M., & Lagrenee, M. (2005). Thermodynamic characterization of metal dissolution and inhibitor adsorption processes in mild steel/2, 5-bis (n-thienyl)-1, 3, 4-thiadiazoles/hydrochloric acid system. *Corros. Sci.*, 47(12) 2915-2931.
30. Li, W. H., He, Q., Zhang, S. T., Pei, C. L., & Hou, B. R. (2008) Some new triazole derivatives as inhibitors for mild steel corrosion in acidic medium. *J. Appl. Electrochem.*, 38, 289-295.
31. Qu, Q., Hao, Z., Jiang, S., Li, L., & Bai, W. (2008) Synergistic inhibition between dodecylamine and potassium iodide on the corrosion of cold rolled steel in 0.1 M phosphoric acid. *Mater. Corros.*, 59 (11) 883–888.
32. Bentiss, F., Traisnel, M., & Lagrenee, M. (2000) The substituted 1, 3, 4-oxadiazoles: a new class of corrosion inhibitors of mild steel in acidic media. *Corros. Sci.*, 42(1) 127-146.
33. Schweinsberg, D. P., George, G. A., Nanayakkara, A. K., & Steinert, D. A. (1988) The protective action of epoxy resins and curing agents—inhibitive effects on the aqueous acid corrosion of iron and steel. *Corros. Sci.*, 28(1) 33-42.
34. Shokry, H., Yuasa, M., Sekine, I., Issa, R. M., El-Baradie, H. Y., & Gomma, G. K. (1998) Corrosion inhibition of mild steel by Schiff base compounds in various aqueous solutions: part 1. *Corro. Sci.*, 40(12) 2173-2186.
35. Singh, A. K., & Quraishi, M. A. (2010) Inhibiting effects of 5-substituted isatin-based Mannich bases on the corrosion of mild steel in hydrochloric acid solution. *J. Appl. Electrochem.*, 40(7) 1293-1306.



© 2017 by the authors; licensee Growing Science, Canada. This is an open access article distributed under the terms and conditions of the Creative Commons Attribution (CC-BY) license (<http://creativecommons.org/licenses/by/4.0/>).